4-1-2004

The Effects of Low-Temperature Dielectronic Recombination on the Relative Populations of the Fe M-Shell States

S. B. Kraemer
NASA Goddard Space Flight Center

Gary J. Ferland
University of Kentucky, gary@uky.edu

J. R. Gabel
NASA Goddard Space Flight Center

The Effects of Low-Temperature Dielectronic Recombination on the Relative Populations of the Fe M-Shell States

Digital Object Identifier (DOI)
http://dx.doi.org/10.1086/382034

The Astrophysical Journal, 604:556–561, 2004 April 1

THE EFFECTS OF LOW-TEMPERATURE DIELECTRONIC RECOMBINATION ON THE RELATIVE POPULATIONS OF THE Fe M-SHELL STATES

S. B. Kraemer,[1] G. J. Ferland,[2] and J. R. Gabel[1,3]
Received 2003 September 23; accepted 2003 December 15

ABSTRACT

We examine the effects of low-temperature, or $\Delta n = 0$, dielectronic recombination (DR) on the ionization balance of the Fe M shell (Fe IX–Fe XVI). Since $\Delta n = 0$ rates are not available for these ions, we have derived estimates based on the existing rates for the first four ionization states of the CNO sequence and newly calculated rates for L-shell ions of third-row elements and Fe. For a range of ionization parameter and column density applicable to the intrinsic absorbers detected in *ASCA*, *Chandra*, and *XMM-Newton* observations of Seyfert galaxies, we generated two grids of photoionization models, with and without DR. The results show that the ionization parameter at which the population of an Fe M-shell ion peaks can increase in some cases by a factor of more than 2 when these rates are included. More importantly, there are dramatic changes in the range in ionization parameter over which individual M-shell ions contain significant fractions of the total Fe (e.g., >10%) in the plasma. These results may explain the mismatch between the range of Fe ionization states detected in the X-ray spectra of Seyfert galaxies, identified by the energies of the M-shell unresolved transition array, and those predicted by photoionization models of the X-ray absorbers that reproduce lines of second- and third-row elements. The results suggest that care should be taken in using third- and fourth-row ions to constrain the physical conditions in photoionized X-ray plasmas until accurate DR rates are available. This underscores the importance of atomic physics in interpreting astronomical spectroscopy.

Subject headings: atomic processes — galaxies: active — plasmas

1. INTRODUCTION

New X-ray observatories such as the *Chandra X-Ray Observatory* and *XMM-Newton* have made high-resolution spectroscopy of active galaxies possible for the first time, allowing the detection of phases of gas that were previously unknown. The physical state of this gas is interpreted by reference to large-scale numerical simulations; hence, it is critical that physical processes that occur in an ionized plasma be fully understood (the main topic of the conference "Spectroscopic Challenges of Photoionized Plasmas" held at the University of Kentucky in 2000 November; Ferland & Savin 2001).

The ionization structure and temperatures in cosmic plasmas depend strongly on ionization and recombination processes. Recombination can occur via radiative recombination, charge transfer, or dielectronic recombination (DR). The DR process involves the capture of a free electron by an ion, resulting in doubly excited recombined species with the electron in an autoionizing state. This is followed either by autoionization (i.e., the reverse process) or the emission of a photon, the latter leaving the recombined ion in a stable state.

There are two varieties of DR. The first involves the capture of the electron to autoionizing states with high principal quantum number, with an accompanying core excitation with a change in principal quantum number $\Delta n > 0$ (e.g., Burgess 1964). This form of DR dominates over radiative recombination at temperatures comparable to the ionization potential, i.e., collisionally ionized plasmas. Nevertheless, terms of the same parity as the ground term exist between the ground state and the first excited state of the opposite parity, and thus a series of autoionizing states converge on these terms (see Nussbaumer & Storey 1983). This results in a second type of DR in which there is no change in the principal quantum number of the excited core, or $\Delta n = 0$, which can proceed at low temperatures for which the thermal energy of the free electron is less than the excitation energy of first resonance of the recombining ion. Low-temperature DR is usually the dominant process in photoionized plasmas, with temperatures typically 5%–10% of the ionization potential, such as those detected in X-ray spectra of Seyfert galaxies (e.g., Reynolds 1997; George et al. 1998; Sako et al. 2000; Kaspi et al. 2001, 2002; Kinkhabwala et al. 2002; Turner et al. 2003).

While low-temperature DR rates have been calculated for a number of abundant second- and a few third-row elements (Nussbaumer & Storey 1983, 1986, 1987), the full set of ionization states have been completed only for second-row elements. One of the difficulties in these calculations is that the rates depend on the accurate determination of the low-level autoionizing states (see Gu 2003). Ali et al. (1991) estimated low-temperature DR rate coefficients for other ions by taking the mean values from the first four ions of C and O calculated by Nussbaumer & Storey (1983), and they demonstrated that the model-predicted emission-line strengths were strongly affected when these rates were introduced. Savin (2000) has shown that uncertainties in DR rates translate into similar uncertainties in predicted ionic column densities, which may hamper the determination of elemental abundance ratios in the intergalactic medium. There has been recent work in determining both high- and low-temperature DR rates for L shell ions (the Li- through Ne-like isoelectronic sequences), both experimentally (Savin et al. 1999, 2002) and computationally (Gu 2003; Badnell et al. 2003), the results of which emphasize

[1] Catholic University of America, and Laboratory for Astronomy and Solar Physics, NASA Goddard Space Flight Center, Code 681, Greenbelt, MD 20771; kraemer@yancey.gsfc.nasa.gov.
[2] Department of Physics and Astronomy, University of Kentucky, Lexington, KY 40506; gary@pa.uky.edu.
[3] University of Colorado, CASA, UCB 389, Boulder, CO 803309-0389; jack.gabel@colorado.edu.

the importance of this process in photoionized plasma. Note that because of the difficulties in calculating the energies of the autoionizing states, experimental results are critical.

On the other hand, there has not been any recent work published on $\Delta n = 0$ rates for M-shell ions (the Na- to Ar-like sequence). This is unfortuitous, since M-shell Fe ions, Fe IX–Fe XVI, contribute strongly to the unresolved transition array (UTA) of inner-shell $n = 2-3$ lines seen in absorption in high-resolution X-ray spectra of several Seyfert galaxies observed with *XMM-Newton* and *Chandra*, such as IRAS 13349+2438 (Sako et al. 2001), NGC 3783 (Blustin et al. 2002; Kaspi et al. 2002; Netzer et al. 2003), Mrk 509 (Pounds et al. 2001; Yaqoob et al. 2003), and NGC 5548 (Steenbrugge et al. 2003, 2004). For N- and M-shell Fe, the UTA features lie between ~15.5 and 17 Å, depending on which ions are present (Behar, Sako, & Kahn 2001). In principal, the UTA can be used to constrain the ionization state of the absorbers, which is especially valuable if the resonance lines from H-, He-, and Li-like C, N, and O are saturated. However, in the case of NGC 3783 (Netzer et al. 2003), the ionization state suggested by the UTA wavelengths seems lower than that predicted by photoionization models generated to fit CNO absorption features and the ionization state/column density of third-row elements such as Si and S. A similar discrepancy appears to be the case for NGC 5548 (Steenbrugge et al. 2004). One of the possible causes Netzer et al. suggested to explain this mismatch is the lack of $\Delta n = 0$ rates for the M-shell Fe ions, which leads to the models predicting the Fe in too high an ionization state (compared to lower Z elements).

In order to explore the effect of $\Delta n = 0$ DR on the M-shell Fe ionization balance, we have adopted the approach described in Ali et al. (1991), adding estimated rate coefficients to the development version of the photoionization code Cloudy (Ferland et al. 1998). In order to gauge the magnitude of the effect, model grids were generated with and without these rates. We also examined the effects of uncertainties in the estimated rates. The model details and results are described below.

2. MODELING METHODOLOGY

Since the mean $\Delta n = 0$ rate coefficients for CNO show an obvious dependence on the residual charge of the ion before recombination (Ali et al. 1991), we would expect a strong charge dependence among the third- and fourth-row M-shell ions. In Figure 1 we show the rates for the L-shell Fe and Ar ions from Gu (2003) for an electron temperature of 4 eV ($\sim 5 \times 10^4$ K), similar to what we would expect in photoionized plasmas in which the iron abundance was peaked at the M shell. Since they span the same range in residual charge, one might expect that the M-shell Fe rates would be similar to the L-shell Ar rates. Hence, we estimated the rate coefficients for iron by generating second-order polynomial fits to the L-shell rates of Fe and Ar and the mean rates for the CNO sequence (Ali et al. 1991), with the functional form

$$R = 1.0 \times 10^{-10}\, 10^{C1+C2xZ+C3xZ^2}\ \mathrm{cm^3\ s^{-1}}, \qquad (1)$$

where Z is the residual nuclear charge of the ion before recombination. The individual fits are shown in Figure 1, and the values of the fit coefficients are listed in Table 1. Since Gu's calculations show a different dependence on Z for different elements within the L shell, we opted not to use this fit for the other third- and fourth-row elements (in some cases, the behavior within the shell cannot be fitted with a second-order

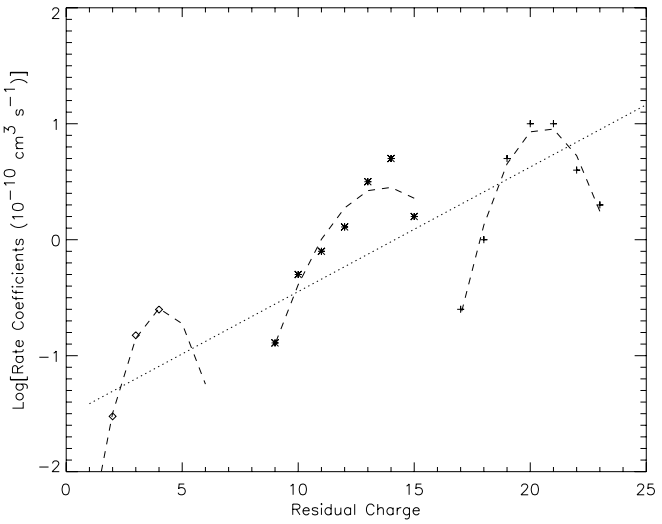

FIG. 1.—The $\Delta n = 0$ DR rate coefficients for L-shell Fe ions (*plus signs*), L-shell Ar ions (*stars*), and the mean rates for the third and fourth ionization states of the CNO ions (*diamonds*) are shown as a function of the residual charge of the ion before recombination. The L-shell rates are those from Gu (2003), for a temperature of 4.0 eV. The dashed lines are second-order polynomial fits for the three shells (N, M, and L), which we used as the functional form for our estimated Fe rate coefficients. The dotted line is a linear fit to the rates, which we used as the functional form for the other third- and fourth-row elements.

polynomial). However, for the sake of completeness, we did estimate $\Delta n = 0$ rates for these ions using a linear fit to a set of data including the Fe and Ar L-shell rates and the mean rates for the CNO sequence (Ali et al. 1991), as shown by the dotted line in Figure 1, with the functional form

$$R = 3.0 \times 10^{-12}\, 10^{0.1Z}\ \mathrm{cm^3\ s^{-1}}. \qquad (2)$$

Since $\Delta n = 0$ DR rates are not fast enough for recombination from closed shells over the range of temperatures that we consider, we did not include estimated DR for those ions. Note that we did not include temperature dependence for our estimated rate coefficients.

To quantify the effects of these missing DR rates, we performed a series of photoionization calculations using the best existing data, but with and without these estimates of the $\Delta n = 0$ DR rates. We did not introduce new high-temperature DR rates, using instead the fit to the rates for Fe given in Arnaud & Raymond (1992). For the models, we assumed a slab geometry, solar abundances (e.g., Grevesse & Anders 1989), a number density of $n_{\mathrm{H}} = 10^8\ \mathrm{cm^{-3}}$, and a total hydrogen column density of $N_{\mathrm{H}} = 1 \times 20^{22}\ \mathrm{cm^{-2}}$, typical of X-ray absorbers; note that the predicted ionization structure is insensitive to n_{H} unless the densities exceed $10^{10}\ \mathrm{cm^{-3}}$. For the spectral energy distribution (SED) of the incident continuum radiation, we assumed a power law of the form $F \propto \nu^{-\alpha}$, where $\alpha = 1$ for $h\nu < 13.6$ eV, 1.4 for 13.6 eV $\leq h\nu \leq$ 600 eV, and 0.8 for $h\nu > 600$ eV. We generated the two sets of

TABLE 1

POLYNOMIAL FIT COEFFICIENTS FOR THE ESTIMATED FE DR RATES

Z	$C1$	$C2$	$C3$
17–23	−52.5073	5.19385	−0.126099
9–15	−10.9679	1.66397	−0.060596
<8	−3.95599	1.61884	−0.194500

models over a range in ionization parameter (number of ionizing photons per nucleon at the illuminated face of the slab) $\log U = -1.0$ to 1.0, in increments of 0.05 dex. Although the mean electron temperatures range from 1.8×10^4 to 4.5×10^5 K, the M-shell Fe ions peak between $\log U = -0.5$ and 0.5, or 3×10^4 K $\lesssim T \lesssim 9.0 \times 10^4$ K, justifying the energy we used in deriving the rate coefficients. Over this temperature range, the DR rates may vary by factors of $\lesssim$a few, which is within the uncertainty quoted above. Note that while T increased slightly when the estimated DR rates were included, the ionic columns for first- and second-row elements remained essentially unchanged.

The predicted ionic column densities for Fe VIII–Fe XVI are shown in Figures 2–4. Since intrinsic X-ray absorption is typically characterized by strong oxygen bound-free edges and absorption lines, we also include the O VI, O VII, and O VIII columns for comparison. As shown in Figure 2, the ionization parameters at which the column densities of Fe VIII, Fe IX, and Fe X peak have all shifted to higher values of U. In the case of Fe X, U has shifted by a factor of $\sim$1.5. More importantly, the range in ionization parameter over which a significant fraction of the total Fe exists as Fe X (i.e., 10%, corresponding to a column density of $\gtrsim 10^{16.6}$ cm^{-2}) has changed from $-0.8 \leq \log U \leq -0.3$ to $-0.8 \leq \log U \leq 0.1$. This suggests that because of $\Delta n = 0$ DR, relatively low ionization states of Fe can contribute significantly to opacity of more highly ionized plasmas than would be predicted using the currently available atomic data. Although the peak shifts are not significant for Fe VIII and Fe IX, the curves show substantially more of these ions at higher values of U. Note that since Fe IX has a closed shell (Ar-like), there is no low-temperature $\Delta n = 0$ process for recombination to Fe VIII, which is produced primarily by radiative recombination. The increase in Fe VIII at higher U is due to the larger fraction of Fe IX, which is produced by DR from Fe X. The structure in the high ionization parameter tails of Fe IX and Fe X is the result of high-temperature DR, although this effect is swamped for Fe X in the models in which $\Delta n = 0$ DR is included. Fe XI–Fe XIII are shown in Figure 3, and for each ion the peaks shift to higher ionization by factors of more than 2, reflecting the large $\Delta n = 0$ rates. Fe XIV–Fe XVI are shown in Figure 4, and the inclusion of $\Delta n = 0$ DR in this case *decreases* the fractional abundances of these ions over much of the adopted range in U, because of the large recombination rates. Nevertheless, $\Delta n = 0$ models predict larger columns of these ions for $\log U \gtrsim 0.7$, as a result of the faster recombination of the L-shell ions.

In order to illustrate the effects of uncertainties in the estimated DR rates, we introduced a "noise factor" by using a random number generator with a Gaussian distribution, with a standard deviation of 0.3 dex, suggested by the largest error in the polynomial fits (see Fig. 1). Furthermore, the DR rates computed by Gu (2003) for L-shell Ar vary by $\sim \pm 0.3$ dex over the range in electron temperatures predicted by our models. Each time Cloudy was run with this option, the recombination coefficient was multiplied by the random number. The scale factor was kept constant for a particular calculation, but different random numbers were used for different calculations. We generated a set of 20 models at each value of U and determined the standard deviation of predicted column densities. In Figure 5 we show the scatter for Fe X at three values of U. Clearly, uncertainties in the rate coefficients have a measurable effect on the predicted ionic columns. Nevertheless, the trend to peak abundance at higher ionization parameter is still obvious, as demonstrated by the overplot of the Fe X columns from the models without the estimated DR.

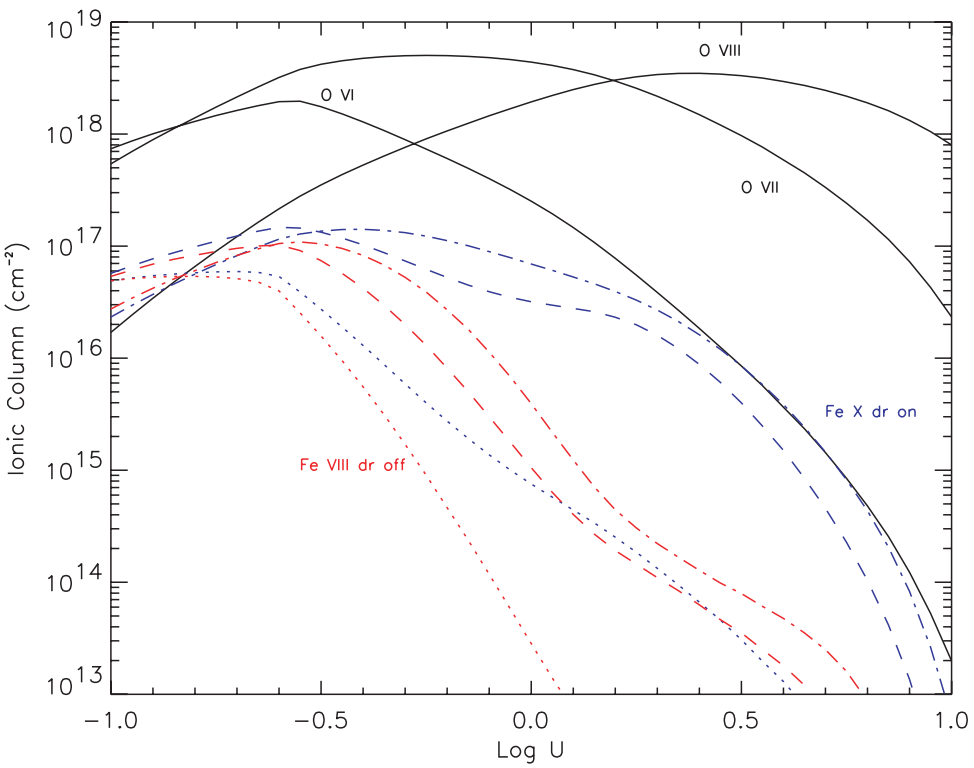

FIG. 2.—Predicted ionic column densities for Fe VIII (*dotted lines*), Fe IX (*dashed lines*), and Fe X (*dash-dotted lines*) are shown as a function of ionization parameter U. The blue lines and red lines are the predictions with and without the estimated $\Delta n = 0$ rates, respectively. The solid black lines are the predicted column densities for O VI, O VII, and O VIII, as indicated. For both sets of models, we assume solar abundances and a hydrogen column density $N_{\rm H} = 10^{22}$ cm^{-2}.

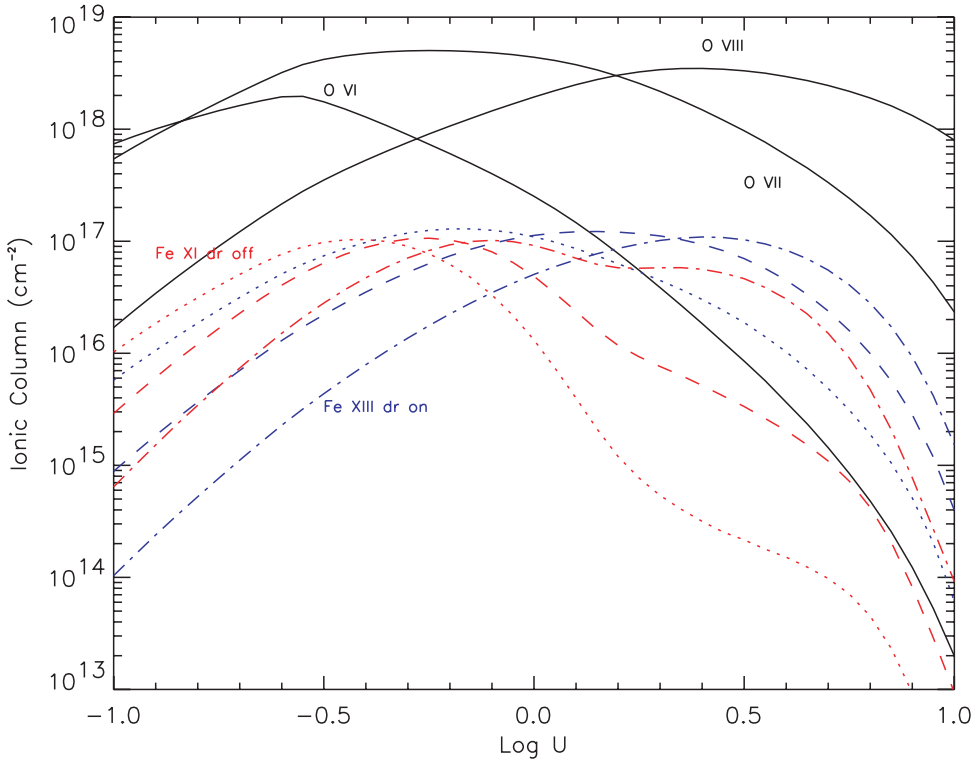

FIG. 3.—Predicted ionic column densities for Fe XI (*dotted lines*), Fe XII (*dashed lines*), and Fe XIII (*dash-dotted lines*) are shown as function of *U*. All other symbols are as defined in Fig. 3.

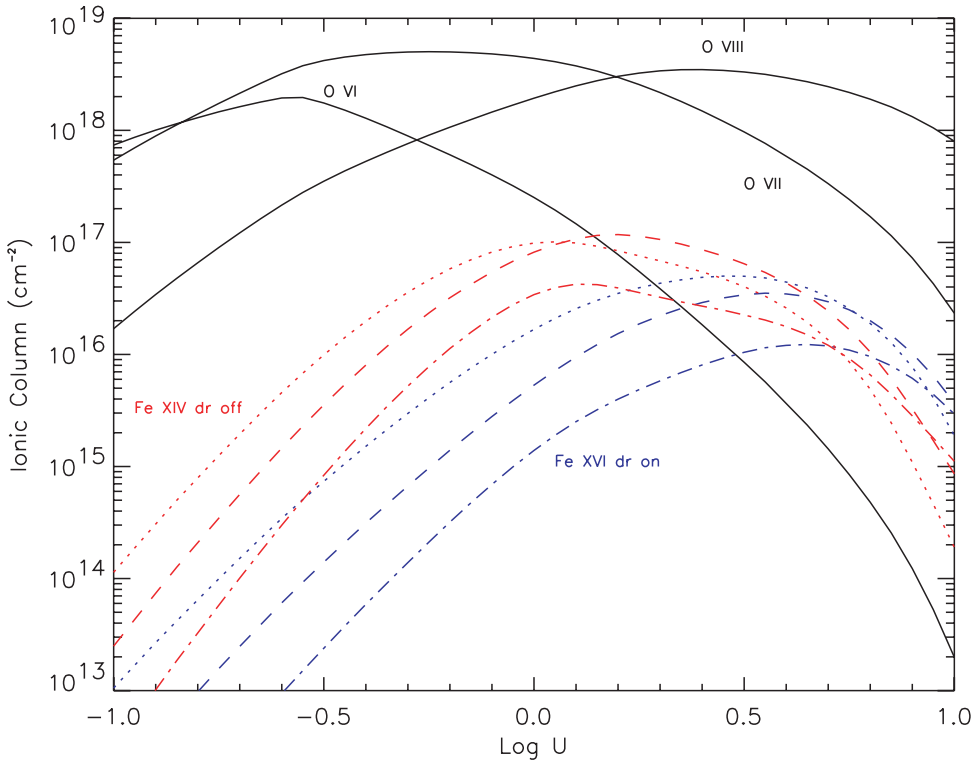

FIG. 4.—Predicted ionic column densities for Fe XIV (*dotted lines*), Fe XV (*dashed lines*), and Fe XVI (*dash-dotted lines*) are shown as function of *U*. All other symbols are as defined for Fig. 3.

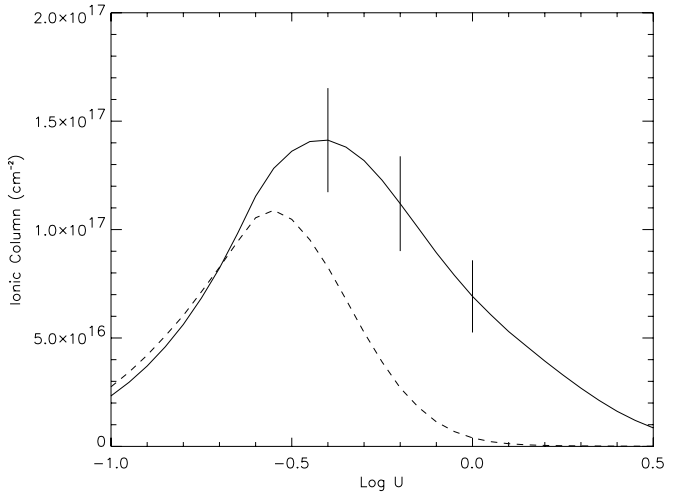

FIG. 5.—Predicted Fe x column density is shown as a function of U. The solid line and dashed line are the predictions with and without the estimated $\Delta n = 0$ rates, respectively. The error bars are included to show the effect of uncertainties in the DR rates, which we model by introducing a random noise factor (see text).

3. CONCLUSIONS

The results of this simple test indicate that the model predictions of the Fe ionization balance depend critically on accurate $\Delta n = 0$ DR rate coefficients. Photoionization models of X-ray absorbers that match spectral features from abundant second-row elements such as C, N, O, and Ne will overpredict the average Fe ionization state if this process is not included. This can be easily demonstrated using Figures 1–3 by selecting an ionization parameter to give the proper ratio of the O VI, O VII, and O VIII column densities and reading off the relative Fe ionic columns for the models with and without the estimated DR. The apparent discrepancy in the ionic states detected in the Fe M-shell UTA in NGC 3783 (Netzer et al. 2003), compared to those predicted by the absorber models, is likely due to the absence of $\Delta n = 0$ rates. To illustrate this point, we regenerated the so-called low-ionization model used by Netzer et al. to fit the soft X-ray absorption and inner-shell Si and S lines detected in a 900 ks merged *Chandra*/High Energy Transmission Grating spectrum of NGC 3783 (see also Kaspi et al. 2002). Following Netzer et al., we assumed the SED described in Kaspi et al. (2001) and set $\log U = -0.26$ and $N_{\rm H} = 10^{21.9}$ cm^{-2} (note that our conversion from the X-ray ionization parameter used by Netzer et al. to the form of U used in Cloudy resulted in a model prediction of slightly higher relative ionization of Si and S than they predicted, which may be due to slight differences in the model SED; in order to reproduce the same columns of Si and S, we adjusted the value of U downward by 10%). The predicted ionic columns for Fe VIII–Fe XII, without $\Delta n = 0$ DR, are given in Table 2, and the combined Fe XI and Fe XII column is ~3.5 greater than the combination of Fe VIII and Fe IX, while the peak ionization state is Fe XI. Since the strongest UTA features for Fe XI and Fe XII lie at 16.16 and 15.98 Å, respectively (Behar et al. 2001), the UTA would peak near 16.1 Å, as described by Netzer et al. Also shown are the predictions for the same model with $\Delta n = 0$ DR included. In this case, the peak ionization state is Fe X, and the total Fe VIII and Fe IX columns are approximately equal to those of Fe XI and Fe XII combined. Since Fe VIII and Fe IX produce their strongest features at 16.89 and 16.51 Å, respectively (Behar et al.), and the profile would be dominated by Fe X (16.34 Å), the predicted UTA will peak near 16.4 Å, as observed. It should also be noted that including the new L-shell rates for third-row elements such as S, Si, and Mg will alter the predicted ionization balance for those elements as well. As noted by Behar & Netzer (2002), inner-shell absorption lines from these ions can be used as effective probes of high-column absorbers. However, care must be taken in using photoionization models to determine ionization states and total column densities of the absorbers using these lines as constraints, at least until a full set of accurate L-shell DR rates have become available.

TABLE 2
PREDICTED Fe M-SHELL COLUMN DENSITIES (cm^{-2}) FOR NGC 3783

Ion	log ($N_{\rm ion}$), No $\Delta n = 0$ DR	log ($N_{\rm ion}$), with $\Delta n = 0$ DR
Fe XIII	16.62	15.90
Fe XII	16.83	16.48
Fe XI	16.88	16.88
Fe X	16.78	17.02
Fe IX	16.52	16.90
Fe VIII	15.81	16.18

NOTE.—Predictions are for the low-ionization component of the X-ray absorber described in Netzer et al. 2003, assuming $\log U = -0.26$, $\log (N_{\rm H}) = 21.90$.

Seyfert galaxies are also strong soft X-ray emission line sources (e.g., Sako et al. 2000; Kinkhabwala et al. 2002; Turner et al. 2003). It will be important to understand the connection between this component and forbidden "coronal" emission lines such as [Fe X] λ6374, [Fe XI] λ7892, [Fe XIV] λ5303, and [S XII] λ7611 (e.g., Kraemer & Crenshaw 2000), especially since the optical/UV spectral images obtained with the *Hubble Space Telescope*/Space Telescope Imaging Spectrograph provide tighter constraints on the spatial extent and kinematic properties of the emission-line gas. Accurate DR rates are crucial for modeling this component and exploring the link between the X-ray and optical emission lines.

While the models generated for this paper clearly illustrate the magnitude of the problem, we are left with the question of how best to proceed in the absence of a full set of $\Delta n = 0$ DR rate coefficients. Our Monte Carlo calculations (see Fig. 5) provide an estimate of the error in the predicted column densities due to the uncertainties in the rate coefficients. In fact, our results suggest that comparisons between calculated and observed column densities be given error bars of ~0.3 dex, assuming that our rates are included in the calculations, because of the uncertainties in the rates and the unmodeled temperature dependence (as suggested by the variations in the published L-shell rates over the range in temperature predicted by our models, e.g., 1.8×10^4 K $\leq T \leq 4.5 \times 10^5$ K). Clearly, using rates estimated from other ions is far better than assuming that the process does not occur, which is what is done when it is neglected. Hence, we suggest that it is best to adopt these estimated rate coefficients with this stated error. Ultimately, new atomic data in general, and DR rates in particular, are needed to reliably compare the ionization of third- and fourth-row elements.

S. B. K. and J. R. G. acknowledge support from NASA grant NAG5-13109 and Smithsonian grant GO2-3138A. S. B. K. thanks Hagai Netzer for useful discussions concerning the Fe UTA lines. We thank an anonymous referee for useful comments.

REFERENCES

Ali, B., Blum, R. D., Bumgardner, T. E., Cranmer, S. R., Ferland, G. J., Haefner, R. I., & Tiede, G. P. 1991, PASP, 103, 1182
Arnaud, M., & Raymond, J. 1992, ApJ, 398, 394
Badnell, N. R., et al. 2003, A&A, 406, 1151
Behar, E., & Netzer, H. 2002, ApJ, 570, 165
Behar, E., Sako, M., & Kahn, S. M. 2001, ApJ, 563, 497
Blustin, A. J., Branduardi-Raymont, G., Behar, E., Kaastra, J. S., Kahn, S. M., Page, M. J., Sako, M., & Steenbrugge, K. C. 2002, A&A, 392, 453
Burgess, A. 1964, ApJ, 139, 776
Ferland, G. J., Korista, K. T., Verner, D. A., Ferguson, J. W., Kingdon, J. B., & Verner, E. M. 1998, PASP, 110, 761
Ferland, G. J., & Savin, D. W., eds. 2001, ASP Conf. Ser. 247, Spectroscopic Challenges of Photoionized Plasmas (San Francisco: ASP)
George, I. M., Turner, T. J., Netzer, H., Nandra, K., Mushotzky, R. F., & Yaqoob, T. 1998, ApJS, 114, 73
Grevesse, N., & Anders, E. 1989, in AIP Conf. Proc. 183, Cosmic Abundances of Matter, ed. C. J. Waddington (New York: AIP), 1
Gu, M. 2003, ApJ, 590, 1131
Kaspi, S., et al. 2001, ApJ, 554, 216
———. 2002, ApJ, 574, 643
Kinkhabwala, A., et al. 2002, ApJ, 575, 732
Kraemer, S. B., & Crenshaw, D. M. 2000, ApJ, 532, 256
Netzer, H., et al. 2003, ApJ, 599, 933
Nussbaumer, H., & Storey, P. J. 1983, A&A, 126, 75
———. 1986, A&AS, 64, 545
———. 1987, A&AS, 69, 123
Pounds, K., Reeves, J., O'Brien, P., Page, K., Turner, M., & Nayakshin, S. 2001, ApJ, 559, 181
Reynolds, C. S. 1997, MNRAS, 286, 513
Sako, M., Kahn, S., Paerels, F., & Liedahl, D. A. 2000, ApJ, 543, L115
Sako, M., et al. 2001, A&A, 365, L168
Savin, D. W. 2000, ApJ, 533, 106
Savin, D. W., et al. 1999, ApJS, 123, 687
———. 2002, ApJ, 576, 1098
Steenbrugge, K. C., Kaastra, J. S., de Vries, C. P., & Edelson, R. 2003, A&A, 402, 477
Steenbrugge, K. C., et al. 2004, A&A, submitted
Turner, T. J., Kraemer, S. B., Mushotzky, R. F., George, I. M., & Gabel, J. R. 2003, ApJ, 594, 128
Yaqoob, T., McKernan, B., Kraemer, S. B., Crenshaw, D. M., Gabel, J. R., George, I. M., & Turner, T. J. 2003, ApJ, 582, 105